QUENCH-LOCA PROGRAM AT KIT AND RESULTS OF THE QUENCH-L0 BUNDLE TEST

J. Stuckert, M. Große, C. Rössger, M. Steinbrück, M. Walter
Karlsruhe Institute of Technology (KIT)
Hermann-von-Helmholtz-Platz 1, 76344 Eggenstein-Leopoldshafen

1. Introduction

The current LOCA criteria and their safety goals are applied worldwide with minor modifications since the USNRC release in 1973. The criteria are given as limits on peak cladding temperature (T_{PCT} ≤ 1200°C) and on oxidation level ECR (equivalent cladding reacted) calculated as a percentage of cladding oxidized (ECR ≤ 17% calculated using Baker-Just oxidation correlation). These two rules constitute the criterion of cladding embrittlement due to oxygen uptake. The results elaborated worldwide in the 1980s and 1990s on Zircaloy-4 (Zry-4) cladding tubes behavior (oxidation, deformation and bundle coolability) under LOCA conditions constitute a detailed data base and an important input for the safety assessment of LWRs. In-pile test data (with burn-up up to 35 MWd/kgU) were consistent with the out-of-pile data and did not indicate an influence of the nuclear environment on cladding deformation.

At high burn-up, fuel rods fabricated from conventional Zry-4 often exhibit significant oxidation, hydriding, and oxide spallation. Thus, many fuel vendors have proposed the use of recently developed cladding alloys, such as M5®, ZIRLO™ and other. Therefore, it is important to verify the safety margins for high burn-up fuel and fuel claddings with new alloys. Due to long cladding hydriding period for the high fuel burn-up, post-quench ductility is strongly influenced not only by oxidation but also hydrogen uptake. The 17% ECR limit is inadequate to ensure post-quench ductility at hydrogen concentrations higher than ≈500 wppm [1]. Due to so called secondary hydriding (during oxidation of inner cladding surface after burst), which was firstly observed in JAEA [2], the hydrogen content can reach 4000 wppm in Zircaloy cladding regions around burst [3].

To investigate the influence of these phenomena on the applicability of the embrittlement criteria for the German nuclear reactors it was decided to perform the QUENCH-LOCA bundle test series at the Karlsruhe Institute of Technology (KIT) in the QUENCH facility. Compared to single-rod experiments, bundle tests have the advantage of studying the mutual interference of rod ballooning among fuel rod simulators as well as the local coolant channel blockages in a more realistic arrangement. The program was started in 2010 with the QUENCH-L0 scoping test used 21 heated rods with as-received Zry-4 claddings [4]. Then advanced claddings (Duplex D4, M5®, ZIRLO™) will be used.

2. QUENCH Facility

The main component of the QUENCH test facility is the test section with the test bundle (Fig. 1). A total of 15 QUENCH high-temperature experiments on severe

accident investigations were performed in this facility between 1997 and 2009 [5]. The last two experiments within this series were conducted with M5® [6] and ZIRLO™ [7] cladding materials.

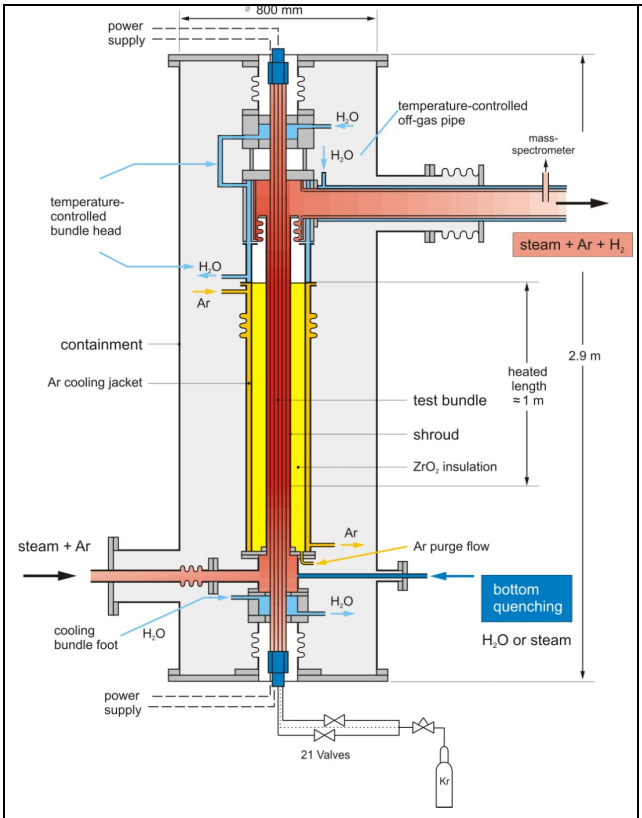

Fig. 1. QUENCH Facility: Containment and test section

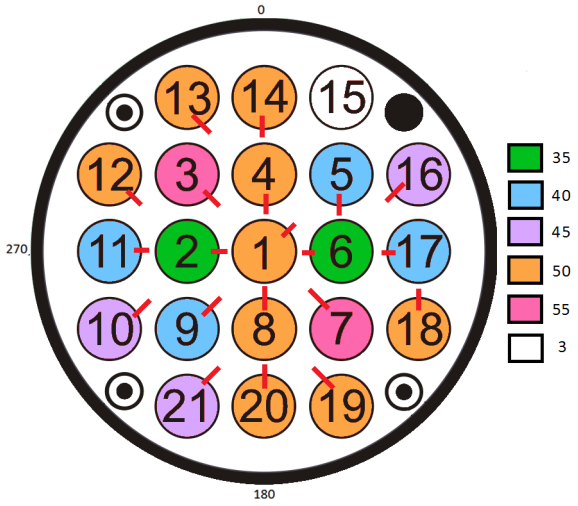

Fig. 2. Pressurization map and burst positions (red bars)

In the forced-convection mode of the QUENCH test facility, superheated steam from the steam generator and superheater together with argon as a carrier gas for off-gas measurements enter the test bundle at the bottom. The gases together with hydrogen produced in the zirconium-steam reaction flow from the bundle outlet at the top through a water-cooled off-gas pipe to the condenser where the steam is separated from the non-condensable gases. The test section has a separate inlet at the bottom to inject water for reflood (quenching).

The QUENCH-LOCA-0 test bundle is approximately 2.5 m long and is made up of 21 fuel rod simulators. This bundle design is applied with a pitch of 14.3 mm. The Zry-4 cladding of the fuel rod simulator has an outside diameter of 10.75 mm and a wall thickness of 0.725 mm. The heating is electric by tungsten heaters with a diameter of 6 mm and a length of 1024 mm, installed in the rod center between bundle elevations 0 and 1024mm. The tungsten heaters are surrounded by annular ZrO_2-TZP pellets, whose heat capacity of 0.9 $J*K^{-1}$/pellet is comparable with the value of 1 J*K 1/pellet for UO_2 pellets. Coated electrodes of molybdenum-copper are connected to the tungsten heaters at one end and to the cable leading to the DC electrical power supply at the other end of the electrodes.

The test bundle is surrounded by a Zr 702 shroud, followed by a ZrO_2 fiber thermal insulation axially extending from the bottom (-300 mm) to the upper end of the heated zone (+1024 mm), and a double-walled cooling jacket. With the shroud's inner diameter ID=80 mm the coolant channel cross section is optimized with respect to

avoid a too large coolant channel area around the outer row of fuel rod simulators. Special corner rods, inserted between bundle and shroud, additionally reduce the coolant channel area to a representative value. These corner rods can be used for withdrawal from the bundle during the test to check the degree of bundle oxidation at specific times.

For temperature measurements the test bundle is equipped with NiCr/Ni thermocouple with stainless steel sheath/MgO insulation and an outside diameter of 1.0 mm. For material compatibility reasons a sleeve of zirconium is swaged onto the thermocouple tip. 56 surface thermocouples are resistance spot- welded to the Zry-4 cladding and distributed at 17 bundle elevations between -250 mm to 1350 mm. 16 other thermocouples have no contact with steam: 3 TCs are installed inside the corner rods and 13 TCs are located at the outer shroud surface.

The gas supply system for individual pressurization of rods consists of pressure controller, 21 valves, 21 pressure transducers, and 21 justified compensation volumes for setting of original volume value of 31.5 cm³ (the compensation is needed because absence of empty plenums inside rod simulators). The gas supply is connected with capillary tubes to each rod at its lower end with drilled copper electrode. Before gas filling the rods and gas supply system were evacuated. At the beginning of experiment, the fuel rod simulators were backfilled with Kr gas to 20 bar. Then, before the transient, they were separately pressurized to the target pressures of 35, 40, 45, 50, and 55 bar as shown in Fig. 2. Different pressure levels were used to investigate the pressure influence on involved processes.

3. Test performance

The experiment started by stabilizing the bundle conditions with an application of electrical bundle power of 4.6 kW (corresponded the linear heat rate of ~1 W/cm) in argon - superheated steam mixture (with effective rates of 0.2 g/s/rod and 0.07 g/s/rod) resulting in maximum bundle temperatures of 800 K. The transient was initiated by rapidly increasing the electrical power to 27 kW (linear heat rate ~6 W/cm) followed by steady increase to 44 kW (linear heat rate ~10 W/cm) within 185 s. During this period the temperatures increased from their initial values to a maximum in excess of 1300 K, as planned. Fig. 3 shows the development of maximum temperature at each elevation (marking TFS x/y means a surface thermocouple for rod x at elevation y). The experiment continued with power decrease to 3.4 kW to simulate decay heat and subsequent (after delay of 30 s) injection of steam at a nominal of 50 g/s at 215 s, resulting in immediate and rapid cooling to about 400 K, which was caused by entrainment of water condensed in steam pipe line. The cooling phase was followed by a second, minor reheating to about 660 K and terminated by 90 g/s water injection at 360 s.

The axial temperature profile in the bundle has a pronounced maximum between 850 and 1050 mm. There is also a radial temperature gradient due to two reasons: 1) radial heat flux to the shroud, 2) electrical power supplied to internal rod group was higher than the power for external group because both DC generators reached current limit (~3600 A) but electrical resistance of 11 external parallel connected rods is lower than for 10 internal rods.

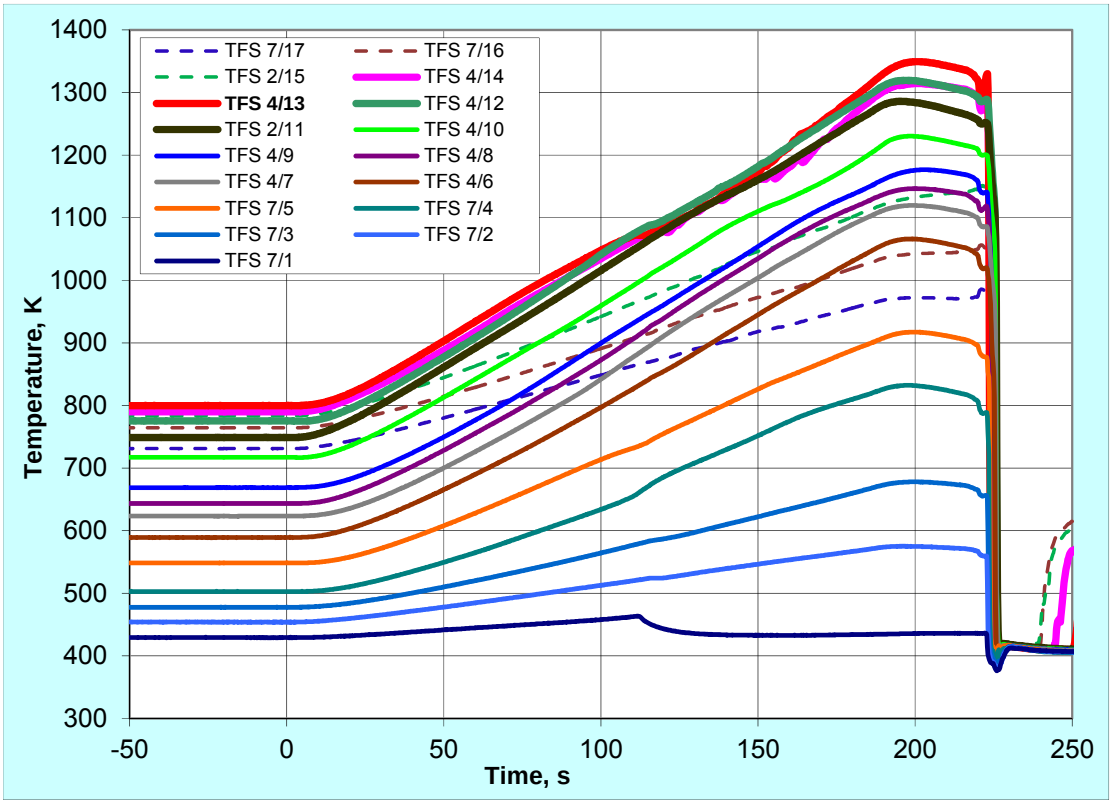

Fig. 3. Rod surface TC readings.

4. Ballooning and burst of claddings.

The increased ductility of claddings during the transient phase resulted in a progressive ballooning and consequent burst of all of the pressurized rods. The first burst occurred 111 s after initiation of transient at about 1069 K at rod #1 which was pre-pressurized to 50 bar. All 20 pressurized rods failed within 63 s. (Fig. 4). The last failed rod was the peripherical rod #10. The temperature range for bursts is estimated from thermocouple readings to be between 1049 and 1141 K. The burst time is mainly controlled by the rod temperature, which has a much stronger influence on the burst time than the internal pressure. The radial burst positions of all rods, except the central one, correspond to the hottest rod region and are directed to the bundle center (Fig. 2). All bursts are axially located between 930 and 1010 mm. The measured burst lengths are between 8 and 20 mm and there is no identifiable dependence on loading internal pressure. No global blockage was formed due to the scattering of the ballooning positions (Fig. 5). All pressurized rods revealed axial contraction by ~10 mm due to Zircaloy anisotropy. No significant rod bending was observed.

The axial and azimutal diameter changes were measured after the test for each pressurized rod for the whole rod length with steps of 1 mm and 1° respectively by means of special laser scanner. On the basis of diameter measurements it was established that the ductile deformation of each rod extends between elevations 250 and 1250 mm. The range of circumferential strains in the burst region was between 25% (rod #10) and 49% (rod #8). The circumferential strain of the central rod was 34%. Extensive data from the laser scanner measurements allows define the degree of the bundle blockage for each elevation. The blockage at all elevations is insignificant due to the relatively wide axial scattering of the maximum ballooning

positions on one hand, and practical absence of touching rods on the other hand. The maximum bundle blockage of 21% was measured at bundle elevation 995 mm.

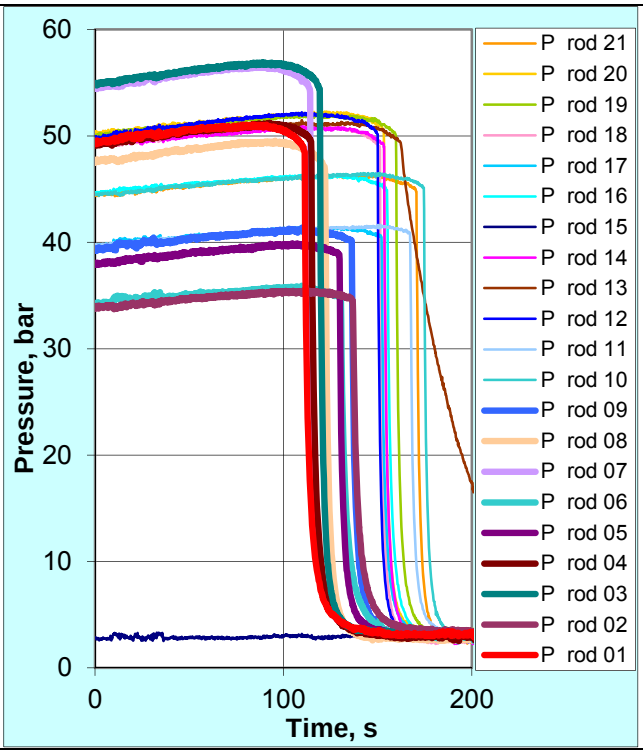

Fig. 4. Internal rod pressures during transient

Fig. 5. Burst region of bundle

5. Investigation of secondary hydrogenation

The metallographic investigation of the cross section of rods at the elevation of the burst middle evidences oxide layer growth at the outer cladding surface as well as oxidation of the inner surface. The boundary of the inner oxidized region was observed at distances 10-20 mm from lower and upper edges of burst. The internal cladding oxidation is caused by steam penetration through the burst opening. It can be assumed that the hydrogen, released during the oxidation of the inner cladding surface, propagated in the gap between cladding and pellet up to boundary of the inner oxidised region. Outside of this region there is no more barrier for the absorption of hydrogen by the metal, and this internally oxidised region should be surrounded by hydrided zones. This assumption was confirmed by neutron radiography, which is a powerful tool for the determination of hydrogen concentration and distribution in zirconium alloys [8]. Hydrogen can be quantitatively and non-destructively determined with a spatial resolution of about 25 µm. The investigations comprise measurements of five internal and five external rods. The radiography of the non-pressurized rod #15 revealed that the effect of the oxide layer is not meaningful. Fig. 6 shows radiographs of the rods #3, #6 and #10. On both sides of the burst positions of internal rods #3 and #6 sloping and bended hydrogen containing darker bands can be clearly seen. The important parameter determining the hydrogen uptake is the time between burst and quenching τ_Q. During part of this time the fill gas flows out of the burst opening. When this process is finished, the steam penetrates into the rod and oxidation of the inner cladding surface takes place in a significant manner. A threshold time seems to exists during which the fill gas flows out. This threshold is between 64 s (rod #19, no hydrogen containing band) and 70 s (rod #14, hydrogen containing band exists). For a quantitative analysis a

neutron tomography was applied. Maximal hydrogen concentrations of about 1330 wppm were measured for hydrogen bands of the central rod.

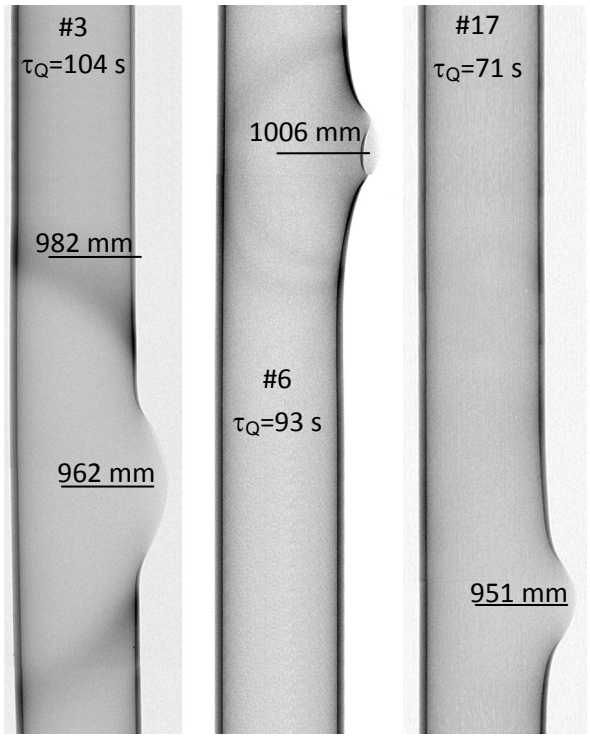

Fig. 6. Hydrogen bands around burst

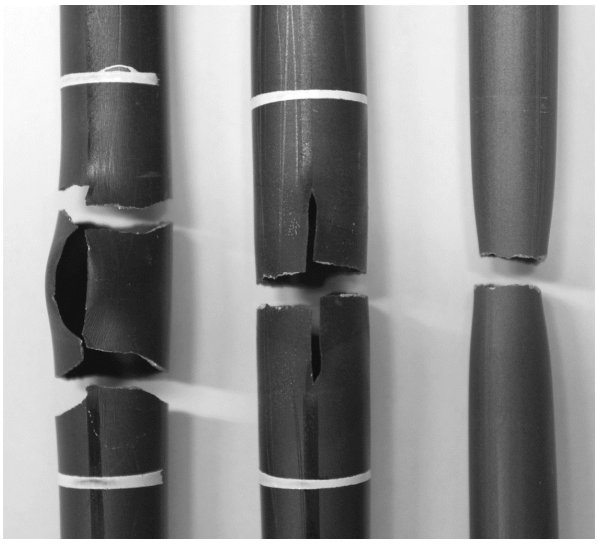

Fig. 7. Three types of cladding rapture

The destructive tensile tests were performed to identify the embrittlement of claddings in dependence on test conditions. These experiments were carried out on longer cladding sections (length L_0 ~ 0.5 m) using the Instron testing machine, equipped with special grip holders with chain link and an optical measurement system (CCD-cameras system). The optical device was used to documentation of rupture, to measurement of the global axial deformation, as well as local axial deformations from defined (marked with white circumferential stripes) cladding sections during a test (Fig. 7). Three types of cladding rupture were indicated: 1) ruptures near to burst opening due to hydrogen embrittlement (5 from 7 tested internal rods), 2) rupture across the burst opening middle due to stress concentration; 3) rupture near end plugs of sample after plastic deformation.

6. Conclusions

The conduct of the QUENCH-L0 test at KIT proved that the QUENCH facility is suitable for LOCA bundle tests.

The data evaluation showed typical ballooning and burst processes for all 20 pressurized rods. All burst cases took place during the transient heating phase at peak bundle temperatures between 1053 und 1133 K.

Measured maximal circumferential strains at burst positions are between 25% und 50%. Maximal blockage of cooling channel is 21% at hottest elevation 995 mm.

Formation of inner oxide layer around burst opening was observed. Neutron radiography showed the formation of bended, not axial symmetric hydrogen

containing bands with a width of about 10 mm at the boundary of cladding inner oxidized area. Formation of these hydrogen bands was observed for rods with time interval between burst and quench initiation of more than 64 s. A hydrogen content up to 1330 wppm at band locations was measured by means of neutron tomography.

The cladding tensile tests showed that the specimens of the inner rod group of the bundle fail mainly within the region of the hydrogen affected zones, whereas claddings of the outer rod group of the bundle fail after necking at significant distances from the ballooning sections.

7. References

[1] H. M. Chung. “Fuel Behavior under Loss-of-Coolant Accident Situations,” Nuclear Engineering and Technology, Vol. 37, No.4 (August 2005).

[2] H. Uetsuka, T. Furuta and S. Kawasaki. “Zircaloy 4 Cladding Embrittlement due to Inner Surface Oxidation under Simulated Loss-of-Coolant Condition,” Journal of Nuclear Science and Technology, Vol. 18[9], p. 705-717 (September 1981).

[3] M. Billone, Y. Yan, T. Burtseva, R. Daum. “Cladding Embrittlement During Postulated Loss-of-Coolant Accidents,” NUREG/CR-6967 (July 2008).

[4] J. Stuckert, M. Große, C. Rössger, M. Steinbrück, M. Walter. „Results of the commissioning bundle test QUENCH-L0 performed under LOCA conditions”. KIT scientific report KIT-SR 7571. Karlsruhe, 2011.

[5] M. Steinbrück, M. Große, L. Sepold, J. Stuckert, „Synopsis and outcome of the QUENCH experimental program,” Nuclear Engineering and Design, Vol. 240, p.1714–1727 (2010).

[6] J. Stuckert, J. Birchley, M. Grosse, B. Jaeckel, M. Steinbrück. „Experimental and calculation results of the integral reflood test QUENCH-14 with M5® cladding tubes,” Annals of Nuclear Energy, Vol. 37, p. 1036–1047 (2010).

[7] J. Stuckert, M. Große, M. Steinbrück, „Experimental Results of Reflood Bundle Test QUENCH-15 with ZIRLO™ Cladding Tubes,” Proceedings of ICAPP’10, San Diego, June 13-17, Paper 10286 (2010).

[8] M. Grosse, G. Kuehne, M. Steinbrueck, E. Lehmann, J. Stuckert, P. Vontobel,: „Determination of the hydrogen uptake of steam-oxidised zirconium alloys by means of quantitative analysis of neutron radiographs,” Journal of Physics Condensed Matter Vol. 20, Issue 10, Article number 104263 (March 2008)